Characteristics of claudin expression in follicle-associated epithelium of Peyer's patches: Preferential localization of claudin-4 at the apex of the dome region

Hiroshi Tamagawa[1) 2)], Ichiro Takahashi[3)], Mikio Furuse[4)], Yuka Yoshitake-Kitano[4)], Shoichiro Tsukita[4)], Toshinori Itoh[2)], Hikaru Matsuda[2)] and Hiroshi Kiyono[1) 5)]

1) Department of Mucosal Immunology, Research Institute for Microbial Diseases, Osaka University

2) Department of Surgery, Osaka University Graduate School of Medicine

3) Department of Preventive Dentistry & Host Defense, Hiroshima Univ. Graduate School of Biomedical Sciences

4) Department of Cell Biology, Faculty of Medicine, Kyoto University Graduate School

5) Division of Mucosal Immunology, Department of Microbiology and Immunology, The Institute of Medical Science, The University of Tokyo

Running title: Claudin-4 expression in Peyer's patch

Corresponding author; Hiroshi Kiyono
Department of Mucosal Immunology
Research Institute for Microbial Diseases, Osaka University
3-1 Yamadaoka, Suita City, Osaka, 565-0871 Japan
Phone; +81-6-6879-8294 Fax; +81-6-6878-6765
e-mail; kiyono@biken.osaka-u.ac.jp

Abstract

Gut-associated lymphoreticular tissue (GALT), such as Peyer's patches (PP) and cecal patches, are important inductive sites for mucosal immune responses. As such, the GALT may have an epithelial barrier different from that of villous epithelium. In this study, we investigated the immunohistochemical distribution of the claudin family and occludin in the follicle-associated epithelium (FAE) of Peyer's patches and cecal patches of murine intestine. Unique profiles of claudin-2, -3, -4 and occludin expression were noted in the tight junctions of the FAE: claudin-4 was preferentially expressed in the apex region; claudin-2 was only weakly expressed on the crypt side of the FAE compared to stronger expression on the crypt side of villous epithelial cells; claudin-3 and occludin were found throughout the dome. These unique expression patterns were present also in cecal patch FAE. We also found that claudin-4 expression in the FAE of Peyer's patches and cecal patches corresponded with the presence of TUNEL-positive apoptotic cells, and Peyer's patch-deficient mice had expression patterns of claudin and occludin in villous epithelia similar to those in wild-type mice. We conclude that claudin-4 expression is preferentially associated with the dome region of FAE, the mucosal inductive site of the murine intestine. In that location and it might correlate with the cell life cycle, help maintain the apex configuration of the dome, or be a factor favoring the uptake of antigens by the FAE.

Abbreviations: FAE; follicle-associated epithelium

GALT; gut-associated lymphoreticular tissue

PP; Peyer's patch

Keywords: claudin

follicle-associated epithelium

occludin

Peyer’s patch

tight junction

Introduction

The intestinal mucosa is covered with one layer of epithelium. Enterocytes are generated from stem cells in the crypts, become mature forms and migrate to the tips of the villi. The cells, which are continually renewed, have a life span of 2-4 days (Creamer, 1967). To maintain homeostasis and preserve the integrity of the epithelial barrier, the intercellular junctional complex, which consists of tight junctions, adherens junctions and desmosomes, is thought to facilitate appropriate communication between outside and inside environments. Of these mechanisms, tight junctions located at the most apical side play a central role in sealing the intercellular space on epithelial sheets (Anderson and Van Itallie, 1995). Several proteins, mainly occludin (Furuse et al, 1993) and claudin (Furuse et al, 1998; Morita et al, 1999), comprise the tight junctions (Mitic and Anderson, 1998). Various cells, organs and parts of tissue have unique distributions of the various claudins. According to a recent report, claudin-2, -3, -4 and –5 are highly expressed in the rat intestine (Rahner et al, 2001).

Peyer's patches (PP) are an important gut-associated lymphoreticular tissue (GALT) and are critical in the priming of antigen-specific Th1/Th2 cells and IgA-committed B cells, with dissemination of the primed lymphocytes to distant mucosal sites for the generation of antigen-specific IgA immune responses. Like other secondary lymphoid tissues, PP contain all the necessary lymphoreticular cells, including antigen-presenting cells (macrophages and dendritic cells), lymphocytes and supporting stromal cells for the induction of antigen-specific humoral and cellular immunity (McGhee and Kiyono, 1999). One of the unique features of this lymphoid tissue is the presence of an epithelium, called follicle-associated epithelium (FAE), which covers the dome of the patches (Owen, 1977; Owen et al, 1991). Furthermore, M cells, one of the major components of the FAE, are key antigen-sampling cells for the delivery of orally encountered antigens to the underlying

antigen-presenting cells (Neutra et al, 1996).

Some intestinal bacteria, e.g. *Salmonella*, can invade the intestinal tract through M cells (Kohbata et al, 1986; Savidge et al, 1991). Two possible pathways for the uptake of these and other luminal antigens have been suggested: a transcellular pathway and a paracellular pathway (Atisook and Madara, 1991; Kops et al, 1996). Some kinds of *Salmonella* reportedly can invade also through villous epithelial cells (Niedergang et al, 2000; Vazquez-Torres et al, 1999); this invasion may be mediated by submucosal dendritic cells, which possess dendrites that extend toward the intestinal lumen between the epithelial cells (Rescigno et al, 2001). Occludin seems to be critical for the maintenance of the tight barrier between enterocytes and dendritic cells. Besides involvement in the formation of tight junctions, the claudin family functions as a receptor for microorganism-derived molecules. For example, *Clostridium perfringens* enterotoxin binds to tight junction strands, especially to the second loop of claudin-3 and -4 (Fujita et al, 2000; Sonoda et al, 1999). These phenomena suggest that bacteria-originated macromolecules can pass through paracellular pathways by modifying tight junctions. Further, it is also possible that the claudin family acts as a signaling receptor for communication between eukaryotic and parakaryotic cells.

This study was aimed at clarifying whether mucosal inductive tissues, such as PP and cecal patches, have tight junction strands in their FAE that differ from those in villous epithelia.

Results

Claudin and occludin expression in murine villous epithelium

We first examined immunohistochemically the expression of claudin and occludin in murine intestinal epithelium. As expected from previous studies in rat intestine, (Rahner et

al, 2001), occludin was expressed throughout the mucosa of the small (jejunum, Fig. 1A-B) and large (cecum, Fig. 1C and rectum, Fig. 1D) intestine. Among claudin family members, claudin-2 was expressed only in the gland crypts of small and large intestines, whereas claudin-3 was expressed in both the villi and the crypts. Claudin-4 was expressed sparsely in villous tips in the small and large intestines. Occludin, like claudin-3, was present on villi and crypts. Whereas claudin-2, claudin-3 and occludin appeared to be localized preferentially on the apical side of the epithelial cells, claudin-4 was expressed stronger on the basolateral sides rather than on the apical sides. Although the expression of claudin-2, -3, and occludin were common in any parts of intestinal epithelia, our findings illustrate the expression of claudin-4 by selective sites, not every tip of villous epithelium.

Unique characteristics of claudin and occludin expression in FAE of PP and cecal patch

Next, we similarly examined the follicle-associated epithelium (FAE) of PP (Fig. 2A, 2B). Occludin and claudin-3 looked expressed on the FAE as well as on the villous epithelium, from the crypt side of the FAE to the tip of the dome. However claudin-2 was faintly expressed in a restricted region near the crypt bases where claudin-2 was well expressed in case of villous epithelium. In contrast, claudin-4 was preferentially expressed in the FAE dome, and its expression was stronger than in villous tips. Next, we examined the distribution of claudins and occludin in the FAE of lymphoid patches present in the cecal wall (Fig. 2C). The expression patterns of these proteins were similar to those in PP: claudin-3 and occludin were expressed throughout the FAE, whereas claudin-2 was only faintly expressed, at crypt bases, and claudin-4 was prominently expressed at the tops of the dome. In comparison to PP, cecal patches had large aggregates with overlying broad areas of epithelium, and claudin-4 was correspondingly extensively expressed.

Moreover, claudin-4 in the FAE was localized not only on the apical side but also on

the basolateral side of epithelial cells (Fig. 2D), whereas in the villous tip it was exclusively expressed in the basolateral. Co-staining with ZO-1 and claudin-4 antibodies made the differences in it more distinguishable. ZO-1 was expressed only in the apical side of the epithelial cell through the dome of the PP. Claudin-4 was found on the apical side as linear signal, besides was found vaguely on the basolateral side of the epithelial cells. These findings illustrate that claudin-4 expression in FAE of PP is distinctively different from that of intestinal villous epithelium. Since PP have a unique architecture (dome) and the special immunologic function of antigen sampling and presentation when compared with villous epithelium, perhaps claudin-4 in GALT helps maintain these unique attributes.

RT-PCR showed claudin-4 expression on the FAE of Peyer's patches

To confirm the interesting findings about preferential claudin-4 expression on the FAE dome obtained from immunohistochemistry, we next examined the expression level of claudin-4 mRNA (Fig. 3). Epithelial cells from jejunum and Peyer's patches were divided into two parts, approximately tip side and crypt side, by means of mechanical isolation manner followed by MACS® cell sorting (see Materials and Methods). Total RNA was isolated from crypt side of FAE [lane 1], tip side of FAE [lane 2], crypt side of villous epithelia [lane 3], and tip side of villous epithelia [lane 4]. The cDNA was prepared respectively and the amount used for each PCR was equalized by control gene (β-actin). Though the level of occludin mRNA expression was similar in each specimen, the level of claudin-4 expression in the villous crypt was found lowered compared with FAE of PP and the epithelia of villous tip. These RT-PCR data also support our immunohistochemical findings.

Possible association between claudin-4 expression and apoptosis of epithelial cells and FAE of GALT

The localization of claudin-4 in villous tip epithelium and the dome FAE of PP and cecal patches reminded us of the distribution of apoptotic cells in these tissues. Thus, we conducted TUNEL staining for the detection of apoptotic cells in the villous epithelium and GALT. Jejunal epithelium had a few TUNEL-positive cells at the apices of villi. TUNEL-positive cells were more numerous in the FAE of PP and cecal patches. Thus, the distribution of TUNEL-positive cells corresponded closely with the distribution of claudin-4 in these various sites (Fig. 4).

Detection of apoptosis in cells of the half top of the villus was compared with anti-claudin-4 staining. In the villous epithelium, claudin-4 positive cells were found 1.6% of the top half of epithelia, while no claudin-4 positive cells were seen in the bottom half of the villi. Accordingly TUNEL positive cells were detected in approximately 0.8±0.32% and 0.1±0.06% of epithelial cells respectively. As to FAE of PP, however, claudin-4 positive cells were detected in 2.1±0.6% of bottom half and in 21.6±5.2% of top half of the FAE of PP. Thus it was shown that FAE of PP had high frequency of both claudin-4 and TUNEL positive cells, especially claudin-4 is expressed preferentially in the top area on the FAE of PP.

Peyer's patch-null and wild-type mice had similar patterns of claudins and occludin expression

Next we asked whether the intestines of PP-null mice and wild-type mice have similar or different expressions of claudin and occludin in the intestinal epithelium. We prepared three different kinds of PP-null mice: lymphotoxin-alpha deficient ($LT\alpha^{-/-}$), cytokine common gamma-chain-deficient ($C\gamma^{-/Y}$), and lymphocyte-deficient (*aly/aly*) mice.

We found no obvious difference in the distribution of the tight-junction components in either the small intestine (Fig. 5) or large intestine (data not shown) between the various PP-null mice and C57BL/6 mice. We looked especially carefully for a minor difference in claudin and occludin expression in the proximal jejunum and distal ileum of the PP-null mice because PP are most prevalent at these sites in normal mice, but we found no difference.

Discussion

In this study, we examined the distribution of claudin-2, -3, -4 and occludin in murine intestine and the GALT PP and cecal patches. The results of our various experiments are summarized in Table 1. The major and potentially important finding was the preferential expression of claudin-4 in the dome area of the GALT follicle-associated epithelium (FAE). In contrast, the expression pattern of other claudins and occludin was similar to that of villous epithelia. In contrast to its sparse expression in the apices of intestinal villi, claudin-4 was prominently expressed in the FAE. Previous studies have shown possible heterogeneity of claudin expression among different locations of tissue or cell type (Furuse et al, 1998; Gow et al, 1999; Morita et al, 1999b; Morita et al, 1999), including a unique distribution in the rat gastrointestinal tract (Rahner et al, 2001). Those studies, though, did not analyze the distribution of claudin and occludin in GALT. The previous workers reported that claudin-2 was expressed in the crypts of small and large intestinal epithelia, while claudin-3 was found in both crypts and tip regions of intestinal epithelia. Further, claudin-4 was expressed on the tip of villous epithelia of small and large intestines (Rahner et al, 2001). In murine intestinal epithelium, we found claudin-2 expressed in crypts, whereas claudin-3 was expressed in villi and crypts. And claudin-4 was expressed in the villous tips just occasionally, not in every tip. Thus, our data in murine intestines generally agree with the results obtained by the analyses of rat intestinal epithelia, except for the

frequency of expression of claudin-4.

The similarity in location of claudin-4 in the epithelium overlying tips of intestinal villi and the FAE of GALT suggests that claudin-4 has a role in the formation and maintenance of the dome or apex shape of the villi and FAE. Villous epithelial cells are generated in the crypts and proceed upward to the villous tips, and FAE cells similarly are generated in crypts and migrate up to the top of domes of PP and cecal patches, i.e., in the hemispherical area. Thus, it seems possible that claudin-4 contributes to maintenance of the hemispherical configuration.

Another possibility is that the expression of claudin-4 is related to the phenomenon of apoptosis since we found a close association between the locations of claudin-4 and apoptotic cells in intestinal villi and the FAE of PP and cecal patches. Also, we noted a correlation between the numbers of TUNEL-positive cells and the expression of claudin-4; claudin-4 was abundant in the FAE of cecal patches, where TUNEL-positive cells were numerous, but was sparse in the villous tips, where apoptotic cells are rare (Hall et al, 1994). We think it possible that claudin-4 is involved in the process of peeling off epithelial sheets of apoptotic enterocytes. None of the previous studies examined a potential relationship between claudin expression and cell life cycle, including apoptosis. Another interesting observation in the present study was that claudin-2 in the jejunum and colorectum was associated with the cells located in the epithelial crypts, in contrast to the location of claudin-4 on the apices of villi and the FAE. Taken together, these findings suggest that intestinal epithelial cells may be able to alter their junctional molecules in accordance with their different life-cycle stages.

Claudin and occludin expression usually is considered representative of tightness of epithelial sheets. However, evidence from this study and other work (Van Itallie et al, 2001) suggests that claudin-4 expression actually may be associated with loosening of

intercellular junctions. The apices of intestinal villi and the FAE are sites where foreign material may enter or be sampled by the gut. For example, some pathogenic microorganisms can invade through the epithelial cells in intestinal villi via intraepithelial dendritic cells (Rescigno et al, 2001; Vazquez-Torres et al, 1999). Since the FAE of GALT, with its associated M cells, is an important antigen-sampling site for the initiation of immune responses (Owen, 1977; Owen et al, 1991), looseness of its intercellular junctions may favor the capturing of antigens. An interesting possibility is that claudin-4 expression contributes to the formation of relatively loose intercellular junctions. In support of this possibility, the overexpression of claudin-4 in claudin-4 transfected Madin-Darby canine kidney (MDCK) cells resulted in increased transepithelial electrical resistance (TER) and an increase in sodium permeability (Van Itallie et al, 2001).

A subset of thymus-derived T cells, i.e., CD8αβ T cells, residing in PP can migrate to intestinal epithelia and become part of the intraepithelial lymphocyte (IEL) pool (Cepek et al, 1994; Shaw et al, 1998). The IELs and their neighboring epithelial cells reciprocally regulate their development and growth via cytokines and corresponding receptor signaling (Fujihashi et al, 1996; Inagaki-Ohara et al, 1997; Yamamoto et al, 1998). Hence, we considered the possibility that some subsets of IEL derived from PP help regulate claudin and occludin expression in the intestinal epithelium. However, we found that claudin expression in the villous epithelium of PP-null mice was no different from that of wild-type mice. Neither did pre-programmed sites for the development of PP have abnormalities in claudin or occludin expression. These findings suggest that PP-derived IELs are not involved in the regulation of claudin and occludin expression. Currently, we are attempting to determine if thymus-independent gut-originated T cells have such a function.

Materials and methods

Animals

C57BL/6 mice and lymphotoxin alpha-deficient mice ($Lt\alpha^{-/-}$) were purchased from Japan CLEA (Tokyo, Japan). Lymphocyte-deficient mice (aly/aly) were purchased from SLC (Tokyo, Japan). Cytokine common gamma-chain-deficient mice ($C\gamma^{-/Y}$) were kindly provided by Dr. Ishikawa, Keio University, and were maintained in the Experimental Animal Facility at Research Institute for Microbial Diseases, Osaka University (Osaka, Japan).

Preparation of specimens

Mice were euthanized with 150 mg/kg body weight of ketamine. The whole gastrointestinal tract then was dissected and extensively washed with cold phosphate-buffered saline (PBS), followed by immersion in Tissue-Tek® O.C.T. Compound (SAKURA Finetechnical Co., Ltd., Tokyo, Japan). The specimens were rapidly frozen in liquid nitrogen for cryosectioning. Cryosections were prepared on a Leica Cryostat CM3050S (Leica Microsystems, Wetzlar, Germany) at –20°C as thin as 6μm. Sections were mounted on glass slides with APS coating (Matsunami Glass Ind., Ltd., Osaka, Japan) and postfixed in 95% ethanol at 4°C for 30 minutes followed by 1-minute acetone fixation. The slides were washed in PBS at 4°C for 10 minutes in preparation of staining.

Antibodies

Rabbit polyclonal anti-mouse claudin-2, -3, -4 and antibodies were raised as described (Furuse et al, 1998). These antibodies specific for the cytoplasmic domains of claudins and occludin were affinity purified on nitrocellulose membranes with GST fusion proteins of respective claudin proteins (Furuse et al, 1999; Morita et al, 1999a). Affinity-purified rabbit monoclonal

antibody against occludin (Zymed Laboratories, South San Francisco, CA) was used for the detection of occludin expression. And rat monoclonal antibody against ZO-1 (Chemicon, Temecula, CA) was used for double immunostaining with other tight junctional antibodies.

Isolation of villous epithelial cells and FAE of Peyer's patches

Single-cell suspensions of epithelial cells were prepared by mechanical and enzymatic dissociation method using type IV collagenase (Sigma, St. Louis, MO) as described previously (Fujihashi et al, 1996; Kawabata et al, 1997; Takahashi et al, 1997). Briefly, after removal of PP, the intestine was opened longitudinally, washed thoroughly, and cut into small fragments. Tip side epithelial cells and intraepithelial lymphocytes (IEL) were removed from intestinal tissue by incubating in RPMI 1640 (Sigma) containing 2% FBS, shaking vigorously, and filtering. After several repetition of this procedure, the specimens were then minced and added to Joklik's modified medium containing collagenase. Crypt side epithelial cells and lamina propria lymphocyte (LPL) were dissociated by stirring at 37°C. Then epithelial cells in respective specimens were isolated using the discontinuous density gradients procedure with Percoll (Amersham Pharmacia Biotech, Uppsala, Sweden). Furthermore CD3e positive or CD19 positive or MHC class-II positive cells were eliminated by magnetic cell sorting (autoMACS®). As to the FAE of Peyer's patches, similar procedures were also performed.

RT-PCR

The mRNA was isolated from MACS®-sorted epithelial cells by using TRIzol reagent (Invitrogen, Carlsbad, CA), treated with DNase I (Invitrogen), and reverse transcribed into cDNA using PCR buffer (Invitrogen), RNase inhibitor (Toyobo, Tokyo, Japan), oligo$(dT)_{16}$ (Invitrogen), Superscript II reverse transcriptase (Invitrogen), and dNTPs (Amersham Biosciences, Uppsala, Sweden). The mixture was incubated at 42°C for 120 min and then heated to 90°C for 5 min. After treatment with

RNase H (Toyobo), the synthesized cDNA and a series of diluted standard oligonucleotides were quantified with a spectrofluorometer using an OliGreen ssDNA Quantification Kit (Molecular Probes, Eugene, OR). PCR amplification from 10 ng of cDNA for each sample was performed with GeneAmp PCR System 9700 (Perkin-Elmer, Branchburg, NJ). RT-PCR was carried out using primer pairs for occludin (forward, 5'-ATTATGGTGCCCGTGTCC-3'; reverse, 5'-GAGTAGGGCTTGTCGTTGCT-3') and claudin-4 (forward, 5'- TGGATGAACTGCGTGGTG-3'; reverse, 5'-GGTTGTAGAAGTCGCGGA TG-3') for 35 cycles (94°C, 45 sec; 52°C, 1 min; 72°C, 1 min). These oligonucleotides were synthesized by Asahi Techno Glass (Chiba, Japan). ß-Actin control sequences were amplified from tissue total RNA reverse transcribed with oligo dT, then PCR amplified with the ß-actin-specific primer (forward, 5'-TAGATGGGCACAGTGTGGG-3'; reverse, 5'-GGCGTGATGGTGGGCATGG-3') for 30 cycles. The amplified products were separated by electrophoresis in 1.8% agarose gel and were visualized with ethidium bromide.

Immunohistochmaical analyses

Immunohistochemical staining for different claudins and occludin was performed by the method previously described (Furuse et al, 1999; Morita et al, 1999a), with minor modification. Fixed cryosections were blocked in PBS containing 1% of bovine serum albumin (Sigma, St. Louis, MO) for 30 minutes at room temperature. The sections were incubated with primary antibodies diluted approximately 1:1000 in the blocking buffer for 30 minutes at room temperature, and then rinsed twice for 5 minutes each in PBS. The sections were further incubated for 30 minutes at room temperature with secondary antibodies: fluorescein isothiocyanate (FITC) conjugated goat anti-rabbit IgG (Chemicon) or Cy-3-conjugated goat anti-rabbit IgG (Jackson ImmunoResearch Laboratories, West Grove, PA). Sections were washed 3 times with PBS and mounted with Immunon^{TM} Perma Fluor Aqueous Mountant (Thermo Shandon, Pittsburgh, PA). As controls, sections were incubated

with primary antibody or secondary antibody only. Specimens were observed using a fluorescence confocal microscopy.

TUNEL staining

Apoptosis in the tissue section was detected by means of the TUNEL method, using ApopTag® Fluorescein *in Situ* Apoptosis Detection Kit (Intergen, Purchase, NY) for fluorescent staining. Cryosections 6 μm thick were applied, and the following procedures were performed per protocol. Briefly, postfix was performed with a mixture of 67% volume of ethanol and 33% volume of acetic acid at –20°C for 15 minutes. After washing with cold PBS, the specimens were incubated with TdT enzyme for 1 hour at 37°C. Finally, the specimens were incubated with secondary antibody conjugated with FITC for 30 minutes at room temperature in the dark, followed by observation using fluorescence microscopy.

Scoring of apoptosis and immunopositive cells

Scoring was performed using confocal microscopy. Longitudinal sections of crypts and villi were selected for scoring on the basis that from the crypto the tip were all in the section and the crypt lumen was visible. Starting at the base of the crypt column, the cells were numbered up each side and the cell positions containing apoptotic fragments or immunopositive cells were recorded. For each experiment, 20 half-crypts per specimen were scored and a distribution of apoptotic fragments cells for each position was obtained. For measurement of apoptosis and claudin expressing cells in murine intestine, the enterocytes in the top one-third of 20 villi per animal were scored. Selected sections were scored independently for a second time. Comparisons of apoptosis and immunopositive values gained by each method were analyzed using Student's *t*-test. A p value less than 0.05 was considered to indicate statistical significance.

Fluorescence Microscopy

Specimens stained with immunofluorescence reagents were examined and recorded under a fluorescence confocal laser scanning microscope (Micro Radiance MR/AG-2; Bio-Rad, Hercules, CA), attached by Olympus BX50 (Olympus Optical Co., Ltd., Tokyo, Japan).

References

Anderson JM, and Van Itallie CM (1995). Tight junctions and the molecular basis for regulation of paracellular permeability. Am J Physiol 269: G467-475.

Atisook K, and Madara JL (1991). An oligopeptide permeates intestinal tight junctions at glucose-elicited dilatations. Implications for oligopeptide absorption. Gastroenterology 100: 719-724.

Cepek KL, Shaw SK, Parker CM, Russell GJ, Morrow JS, Rimm DL, and Brenner MB (1994). Adhesion between epithelial cells and T lymphocytes mediated by E- cadherin and the alpha E beta 7 integrin. Nature 372: 190-193.

Creamer B (1967). The turnover of the epithelium of the small intestine. Br Med Bull 23: 226-230.

Fujihashi K, Kawabata S, Hiroi T, Yamamoto M, McGhee JR, Nishikawa S, and Kiyono H (1996). Interleukin 2 (IL-2) and interleukin 7 (IL-7) reciprocally induce IL-7 and IL-2 receptors on gamma delta T-cell receptor-positive intraepithelial lymphocytes. Proc Natl Acad Sci U S A 93: 3613-3618.

Fujita K, Katahira J, Horiguchi Y, Sonoda N, Furuse M, and Tsukita S (2000). Clostridium perfringens enterotoxin binds to the second extracellular loop of claudin-3, a tight junction integral membrane protein. FEBS Lett 476: 258-261.

Furuse M, Fujita K, Hiiragi T, Fujimoto K, and Tsukita S (1998). Claudin-1 and -2: novel integral membrane proteins localizing at tight junctions with no sequence similarity to occludin. J Cell Biol 141: 1539-1550.

Furuse M, Hirase T, Itoh M, Nagafuchi A, Yonemura S, and Tsukita S (1993). Occludin: a novel integral membrane protein localizing at tight junctions. J Cell Biol 123: 1777-1788.

Furuse M, Sasaki H, and Tsukita S (1999). Manner of interaction of heterogeneous claudin species within and between tight junction strands. J Cell Biol 147: 891-903.

Gow A, Southwood CM, Li JS, Pariali M, Riordan GP, Brodie SE, Danias J, Bronstein JM, Kachar B, and Lazzarini RA (1999). CNS myelin and sertoli cell tight junction strands are absent in Osp/claudin-11 null mice. Cell 99: 649-659.

Hall PA, Coates PJ, Ansari B, and Hopwood D (1994). Regulation of cell number in the mammalian gastrointestinal tract: the importance of apoptosis. J Cell Sci 107: 3569-3577.

Inagaki-Ohara K, Nishimura H, Mitani A, and Yoshikai Y (1997). Interleukin-15 preferentially promotes the growth of intestinal intraepithelial lymphocytes bearing gamma delta T cell receptor in mice. Eur J Immunol 27: 2885-2891.

Kawabata S, Boyaka PN, Coste M, Fujihashi K, Hamada S, McGhee JR, and Kiyono H (1997). A novel alkaline phosphatase-based isolation method allows characterization of intraepithelial lymphocytes from villi tip and crypt regions of murine small intestine. Biochem Biophys Res Commun 241: 797-802.

Kohbata S, Yokoyama H, and Yabuuchi E (1986). Cytopathogenic effect of Salmonella typhi GIFU 10007 on M cells of murine ileal Peyer's patches in ligated ileal loops: an ultrastructural study. Microbiol Immunol 30: 1225-1237.

Kops SK, Lowe DK, Bement WM, and West AB (1996). Migration of Salmonella typhi through intestinal epithelial monolayers: an in vitro study. Microbiol Immunol 40: 799-811.

McGhee J, and Kiyono H (1999), The mucosal immune system. In: Paul WE, Paul WEs. Fundamental Immunology, 4th edition edition, Vol Philadelphia: Lippincott-Raven Publishers, 909/945.

Mitic LL, and Anderson JM (1998). Molecular architecture of tight junctions. Annu Rev Physiol 60: 121-142.

Morita K, Furuse M, Fujimoto K, and Tsukita S (1999a). Claudin multigene family encoding four-transmembrane domain protein components of tight junction strands. Proc Natl Acad Sci U S A 96: 511-516.

Morita K, Sasaki H, Fujimoto K, Furuse M, and Tsukita S (1999b). Claudin-11/OSP-based tight junctions of myelin sheaths in brain and Sertoli cells in testis. J Cell Biol 145: 579-588.

Morita K, Sasaki H, Furuse M, and Tsukita S (1999c). Endothelial claudin: claudin-5/TMVCF constitutes tight junction strands in endothelial cells. J Cell Biol 147: 185-194.

Neutra MR, Frey A, and Kraehenbuhl JP (1996). Epithelial M cells: gateways for mucosal infection and

immunization. Cell 86: 345-348.

Niedergang F, Sirard JC, Blanc CT, and Kraehenbuhl JP (2000). Entry and survival of Salmonella typhimurium in dendritic cells and presentation of recombinant antigens do not require macrophage-specific virulence factors. Proc Natl Acad Sci U S A 97: 14650-14655.

Owen RL (1977). Sequential uptake of horseradish peroxidase by lymphoid follicle epithelium of Peyer's patches in the normal unobstructed mouse intestine: an ultrastructural study. Gastroenterology 72: 440-451.

Owen RL, Piazza AJ, and Ermak TH (1991). Ultrastructural and cytoarchitectural features of lymphoreticular organs in the colon and rectum of adult BALB/c mice. Am J Anat 190: 10-18.

Rahner C, Mitic LL, and Anderson JM (2001). Heterogeneity in expression and subcellular localization of claudins 2, 3, 4, and 5 in the rat liver, pancreas, and gut. Gastroenterology 120: 411-422.

Rescigno M, Urbano M, Valzasina B, Francolini M, Rotta G, Bonasio R, Granucci F, Kraehenbuhl JP, and Ricciardi-Castagnoli P (2001). Dendritic cells express tight junction proteins and penetrate gut epithelial monolayers to sample bacteria. Nat Immunol 2: 361-367.

Savidge TC, Smith MW, James PS, and Aldred P (1991). Salmonella-induced M-cell formation in germ-free mouse Peyer's patch tissue. Am J Pathol 139: 177-184.

Shaw SK, Hermanowski-Vosatka A, Shibahara T, McCormick BA, Parkos CA, Carlson SL, Ebert EC, Brenner MB, and Madara JL (1998). Migration of intestinal intraepithelial lymphocytes into a polarized epithelial monolayer. Am J Physiol 275: G584-591.

Sonoda N, Furuse M, Sasaki H, Yonemura S, Katahira J, Horiguchi Y, and Tsukita S (1999). Clostridium perfringens enterotoxin fragment removes specific claudins from tight junction strands: Evidence for direct involvement of claudins in tight junction barrier. J Cell Biol 147: 195-204.

Takahashi I, Kiyono H, and Hamada S (1997). CD4+ T-cell population mediates development of inflammatory bowel disease in T-cell receptor alpha chain-deficient mice. Gastroenterology 112: 1876-1886.

Van Itallie C, Rahner C, and Anderson JM (2001). Regulated expression of claudin-4 decreases paracellular conductance through a selective decrease in sodium permeability. J Clin Invest 107: 1319-1327.

Vazquez-Torres A, Jones-Carson J, Baumler AJ, Falkow S, Valdivia R, Brown W, Le M, Berggren R, Parks WT, and Fang FC (1999). Extraintestinal dissemination of Salmonella by CD18-expressing phagocytes. Nature 401: 804-808.

Yamamoto M, Fujihashi K, Kawabata K, McGhee JR, and Kiyono H (1998). A mucosal intranet: intestinal epithelial cells down-regulate intraepithelial, but not peripheral, T lymphocytes. J Immunol 160: 2188-2196.

Table 1.

A summary for the expression pattern of claudin-2, -3, -4 and occludin in murine intestinal epithelia and FAE of GALT

animal	tissue	claudin-2	claudin-3	claudin-4	occludin
C57BL/6	jejunum	+ (crypt)	++	± (tip)	++
	colorectum	+ (crypt)	++	± (tip)	++
	PP (FAE)	-/±	+	++ (tip)	+
	Cecal patch (FAE)	-/±	+	++ (tip)	+
$LT\alpha^{-/-}$	jejunum	+ (crypt)	++	± (tip)	++
$C\gamma^{-/Y}$	jejunum	+ (crypt)	++	± (tip)	++
aly/aly	jejunum	+ (crypt)	++	± (tip)	++

-: no expression

±: occasionally or weakly expressed

+: always expressed

++: always and strongly expressed

Figure legends

Figure 1.

Claudin and occludin expression in villous epithelia of murine jejunum, cecum and rectum

Immunohistochemical staining of claudin-2, -3, -4 and occludin in murine jejunum [A: low magnification, B: high magnification] cecum [C] and rectum [D]. Specimens were cryosectioned 6 μm thick and stained with primary polyclonal antibodies (pAb) specific for the respective claudin and occludin, followed by secondary antibodies conjugated with FITC or Cy-3. Claudin-2 is expressed in the crypt region of jejunal, cecal and rectal glands, whereas claudin-3 is expressed in both crypts and villi. Claudin-4 is present sparsely on villous tip cells in the small and large intestines. Occludin, like claudin-3, is expressed by both crypt cells and villous cells. Claudin-2, claudin-3 and occludin are expressed on the apical side of the epithelium, but claudin-4 is expressed stronger on the basolateral sides rather than on the apical sides of epithelial cells. And in some cases, claudin-4 is seen around some enterocytes in a U-shaped pattern as if associated with apoptotic cells that have just peeled off. Yellow arrowheads indicate examples of claudin-4 positive epithelial cells.

Figure 2.

Claudin expression in Peyer's patches and cecal patches

[A-C] Immunohistochemical staining of claudin-2, -3, -4 and occludin in murine Peyer's patch in jejunum [A, B] and cecal patch[C]. Claudin-3 and occludin are expressed through the FAE. Claudin-2 is just faintly expressed in the restricted region near the crypt. Claudin-4 is preferentially expressed in the tip of the FAE dome compared with villous epithelium. The expression patterns of the claudins and occludin in the FAE are similar between PP and the cecal patches. Yellow arrowheads indicate examples of claudin-4

positive epithelial cells. [D] Co-staining of PP with ZO-1 and claudin-4 antibodies. There is some difference in the localization between the tight junction relating proteins. ZO-1 is expressed only in the apical side of the epithelial cell of the PP. Claudin-4 is expressed in the apical side as linear signal, and is found vaguely in the basolateral side of the epithelial cell. All the specimens are 6μm in thick. Red signals represent ZO-1 (Cy-3), green represent claudin-4 (FITC), and the merge pictures are shown.

Figure 3.

Semiquantative RT-PCR for occludin and claudin-4 mRNA on MACS®-sorted epithelial cells

Epithelial cells from jejunum and Peyer's patches were divided into two parts, approximately tip side and crypt side, by means of mechanical isolation manner followed by MACS® cell sorting (see Materials and Methods). Total RNA was isolated from crypt side of FAE [lane 1), tip side of FAE [lane 2], crypt side of villi [lane 3], tip side of villi [lane 4]. The cDNA was prepared respectively and the amount used for each PCR was equalized by control gene (β2m). The level of occludin mRNA expression is similar in each sample, however the level of claudin-4 expression in the villous crypt is found lowered compared with FAE of Peyer's patch and the epithelia of villous tip. The amplification fragments were visualized on 1.8% agarose gel using ethidium bromide.

Figure 4.

Relationship of claudin-4 expression and TUNEL staining

TUNEL staining of 6-μm thick cryosections of [A] jejunal villi, [B] PP. [A] In the jejunum, a few TUNEL-positive cells (red arrows) are occasionally present in villous tips, where

claudin-4 expression also is present. [B] Claudin-4 expression in the FAE of PP is present in the top area of the domes, corresponding to the presence of TUNEL-positive cells. [C] Quantification of claudin-4 positive cells and TUNEL positive cells per villus or per FAE of Peyer's patch. These FAE has high frequency of both claudin-4 and TUNEL positive cells, especially claudin-4 is expressed preferentially in the top area on the FAE of Peyer's patch.

Figure 5.

Claudin expression in villous epithelium of PP-null mice

Immunohistochemical staining of claudin-2, -3, -4 and occludin in the small intestine of PP-null mice. Three different kinds of PP-null mice were examined: [A] Lymphotoxin-alpha deficient ($LT\alpha^{-/-}$), [B] common gamma-chain deficient ($C\gamma^{-/Y}$) and [C] lymphocyte deficient (aly/aly). All the specimens were cryosections of jejunum. There is no significant difference in the expression pattern of claudins and occludin in the PP-null mice and wild-type mice: claudin-2 is present in the crypts, claudin-3 and occludin throughout the glands, and claudin-4 only occasionally in villous tips. In the large intestine also, the expression of the claudins and occludin was similar in the PP-null and wild type mice (data not shown). Yellow arrowheads indicate examples of claudin-4 positive epithelial cells.

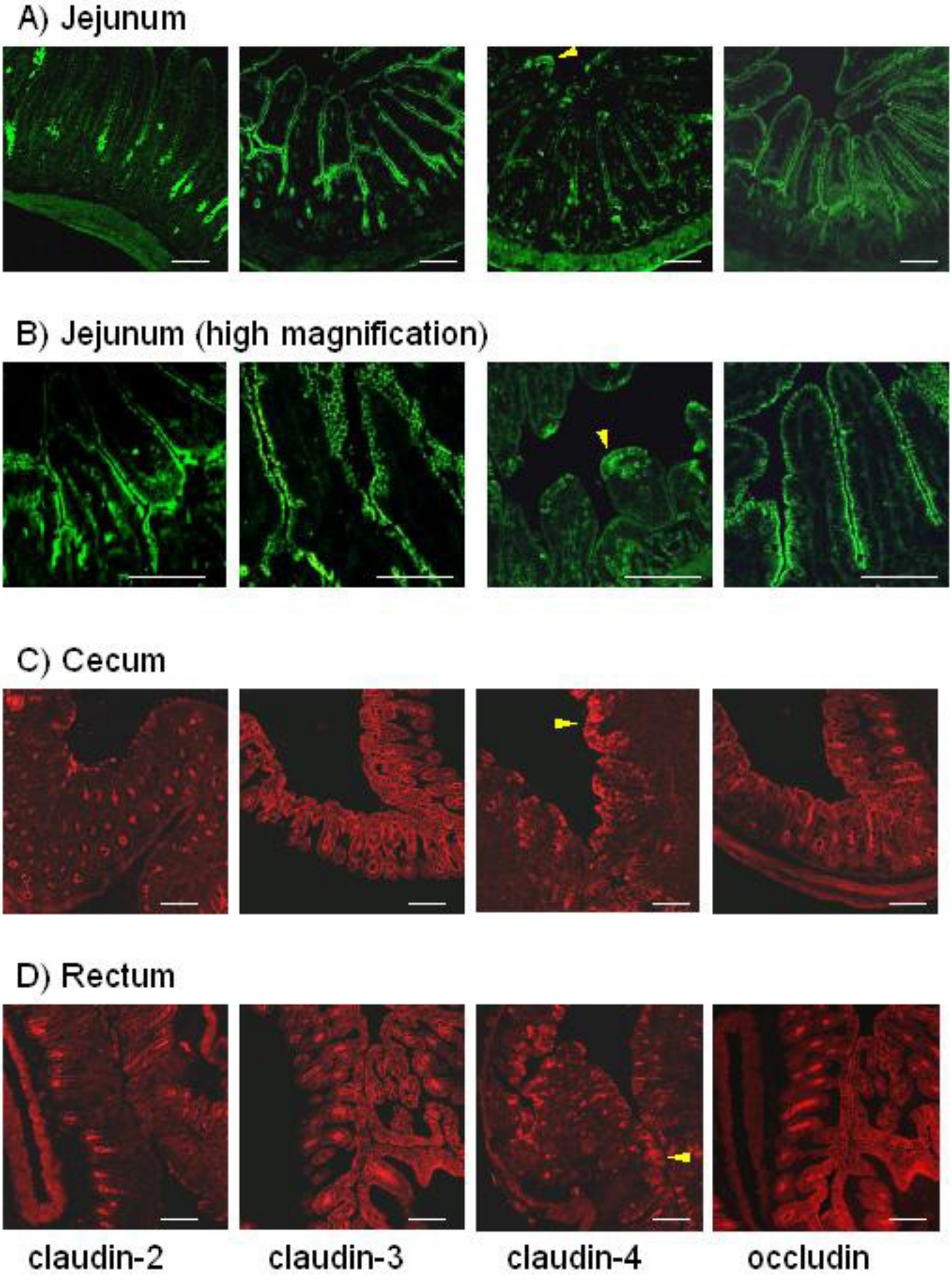
A) Jejunum
B) Jejunum (high magnification)
C) Cecum
D) Rectum
claudin-2
claudin-3
claudin-4
occludin
Bar indicates 200μm

Fig. 1

A) Peyer's patch

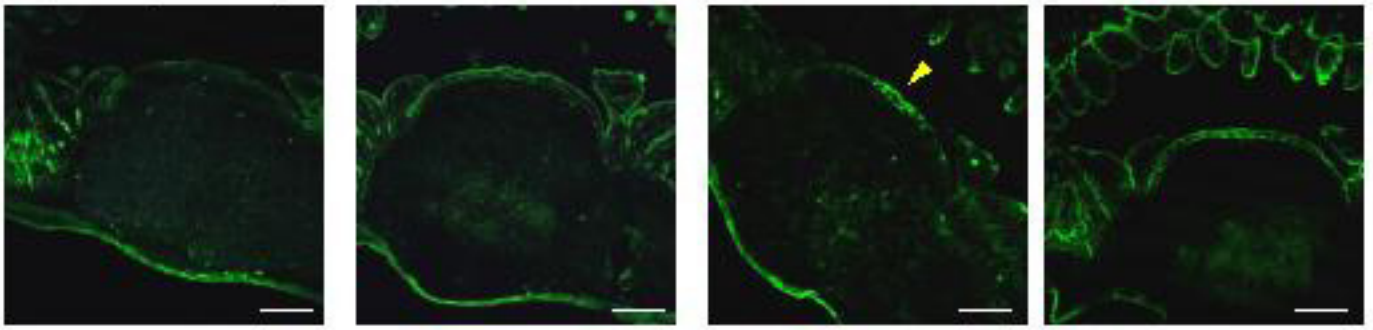

B) Peyer's patch (high magnification)

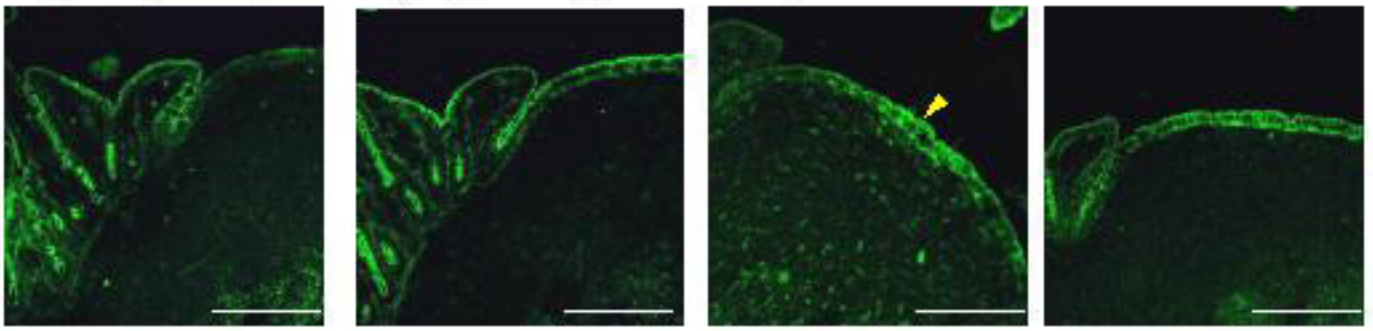

C) Cecal patch

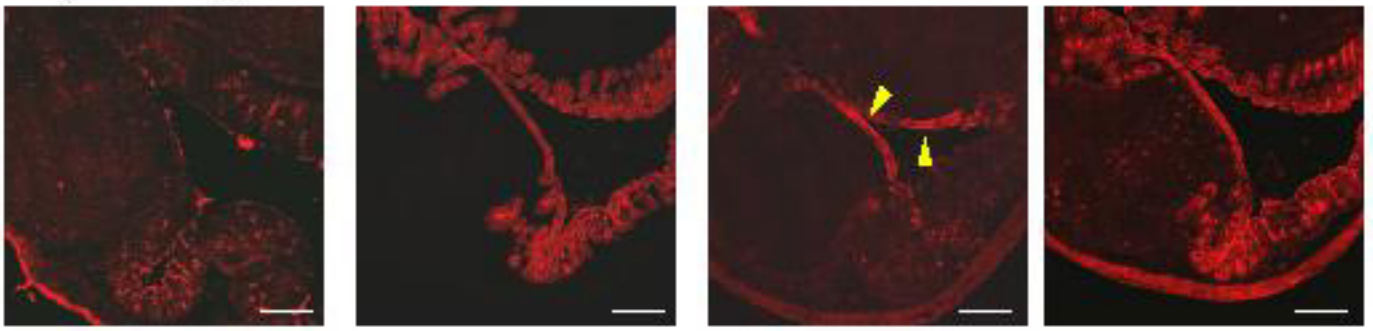

claudin-2 claudin-3 claudin-4 occludin

Bar indicates 200μm

Fig. 2

D) Claudin-4 expression in FAE

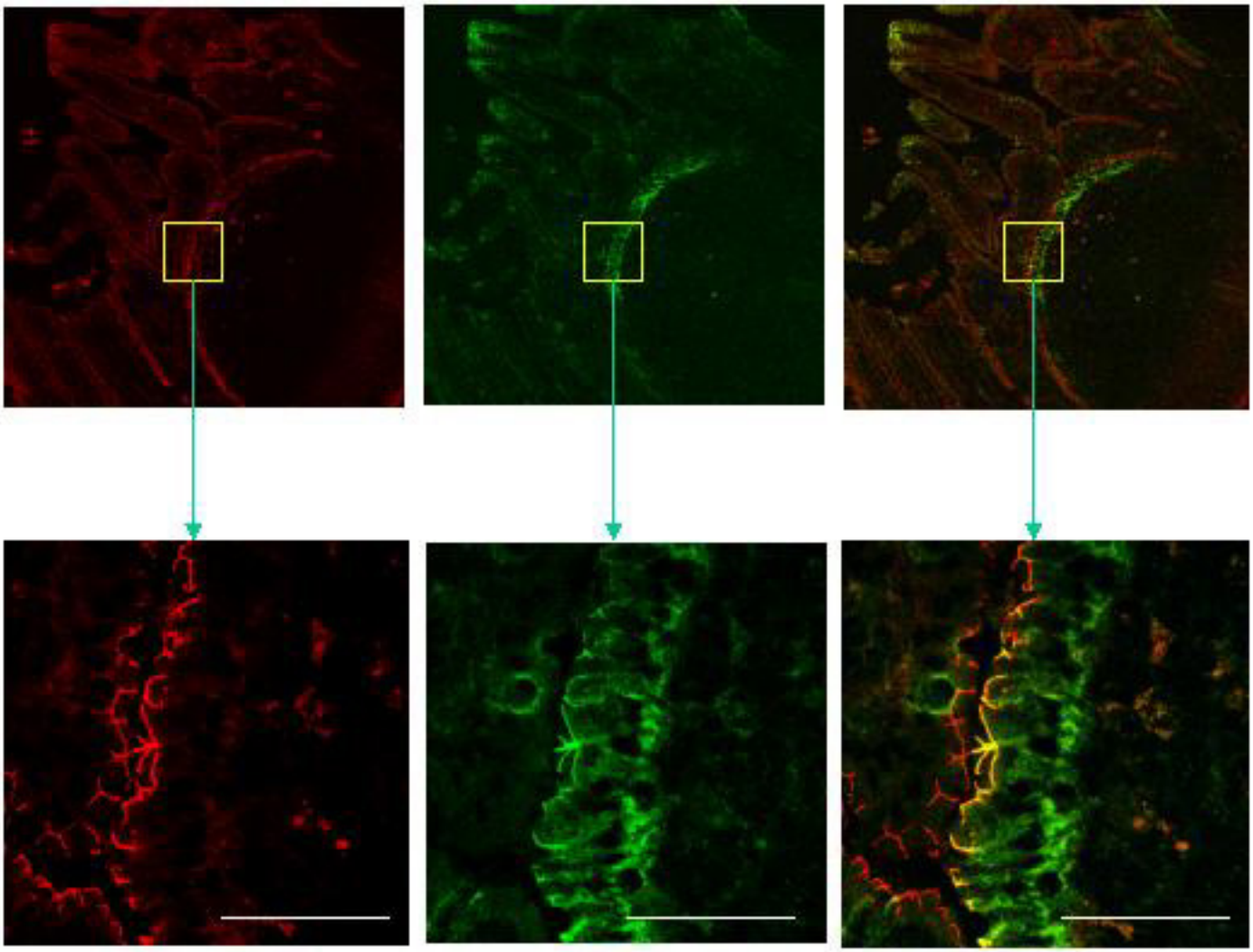

ZO-1 Cy-3 claudin-4 FITC merge

– indicates 50μm

Fig. 2

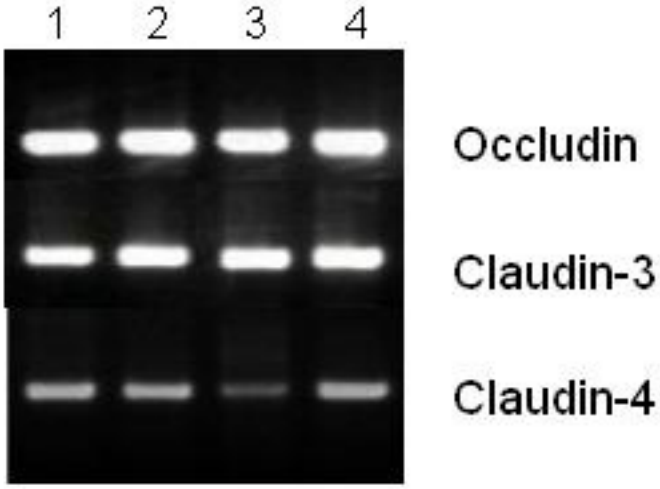

RT-PCR
Lane 1: FAE cells (crypt side)
Lane 2: FAE cells (tip side)
Lnae 3: jejunal EC (crypt side)
Lane 4: jejunal EC (tip side)

Fig. 3

A) Villous Epithelium (Jejunum)

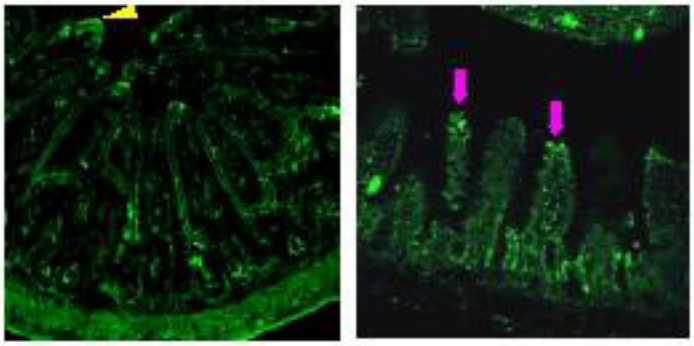

B) Peyer's patch (Jejunum)

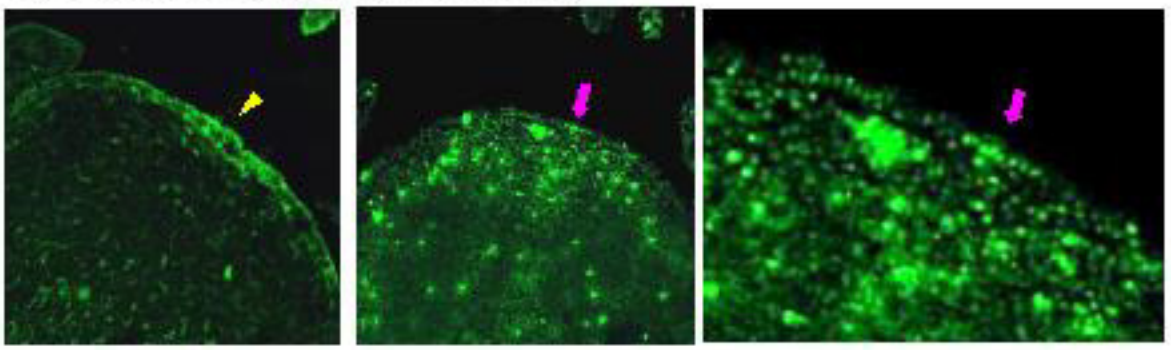

C) Quantification of claudin and TUNEL positive cells

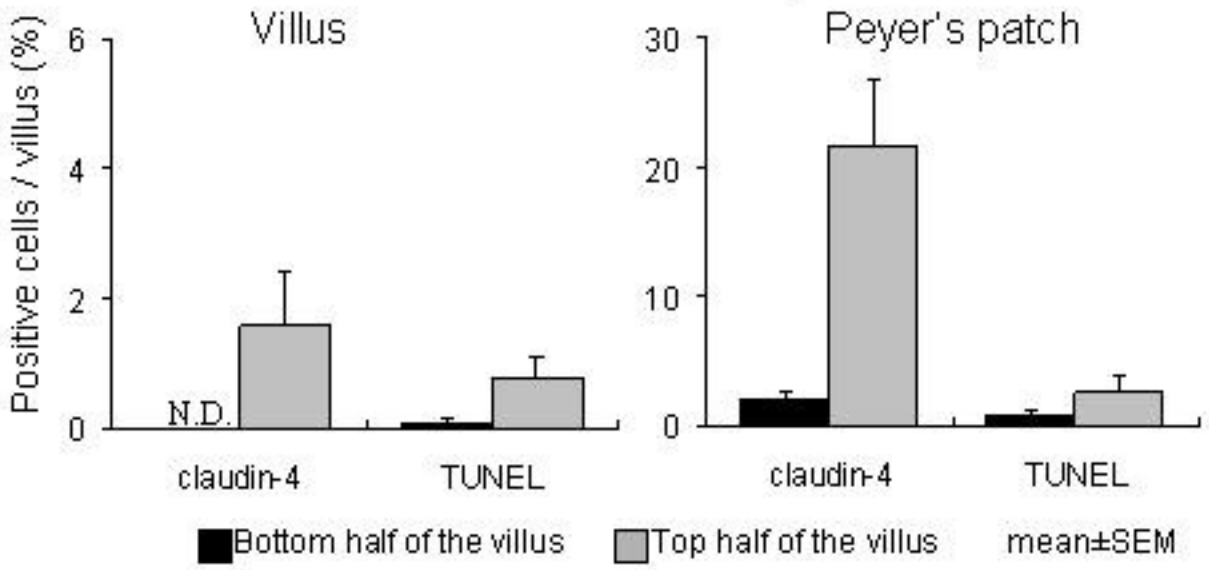

Fig. 4

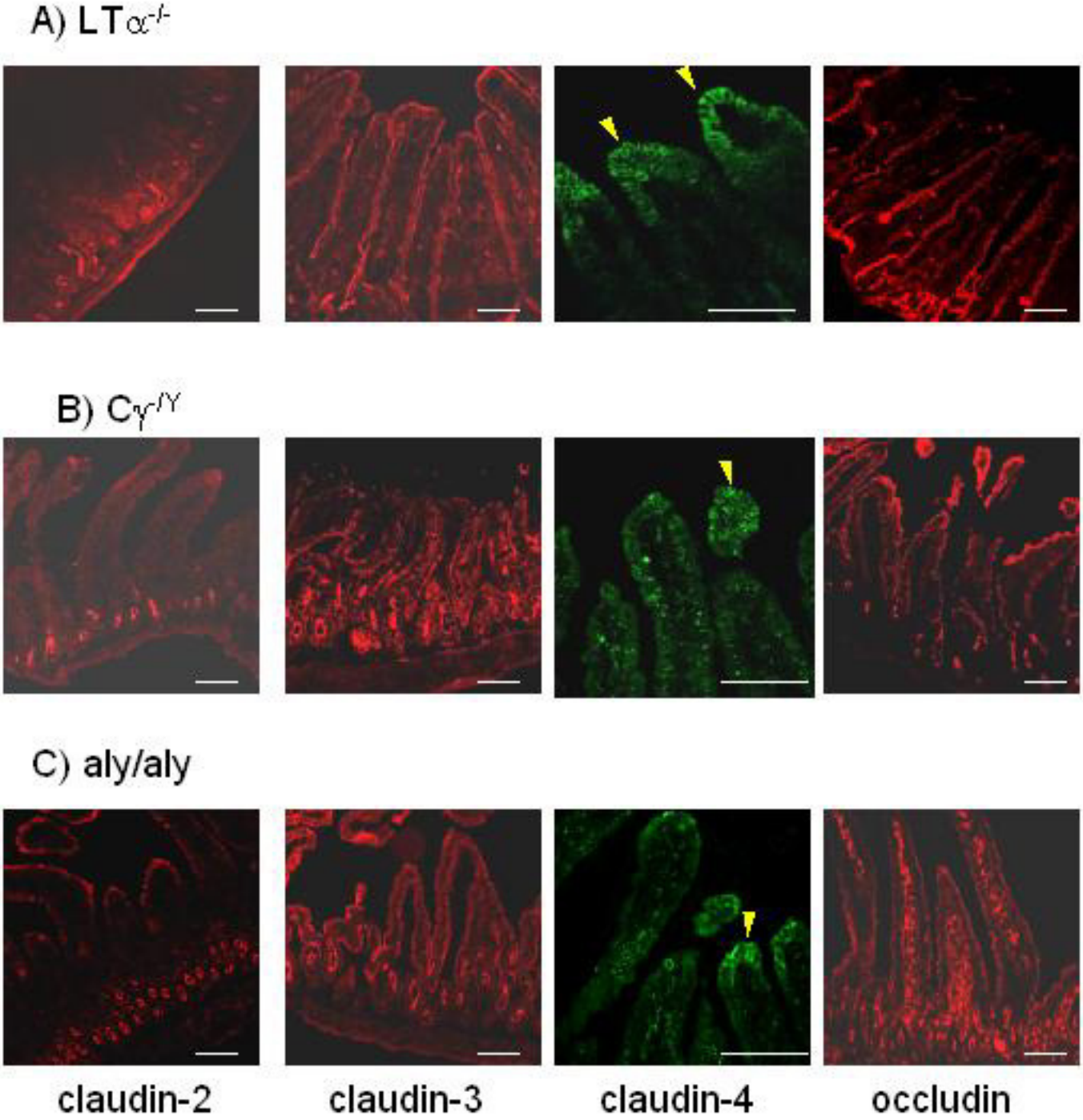
A) LTα-/-
B) Cγ-/Y
C) aly/aly
claudin-2
claudin-3
claudin-4
occludin
Bar indicates 100μm

Fig. 5